Journal of Sound and Vibration (1993) **162**(2), 323–332

DYNAMIC INSTABILITY OF LAYERED ANISOTROPIC CIRCULAR CYLINDRICAL SHELLS, PART II: NUMERICAL RESULTS

A. ARGENTO

Department of Mechanical Engineering, University of Michigan–Dearborn, Dearborn, Michigan 48128-1491, *U.S.A.*

AND

R. A. SCOTT

Department of Mechanical Engineering and Applied Mechanics, University of Michigan, Ann Arbor, Michigan 48109-2121, *U.S.A.*

(*Received* 12 *December* 1989, *and in final form* 25 *November* 1991)

Numerical results for the parametric resonance response of layered anisotropic circular cylindrical shells are presented based on a theoretical development given in part I [1]. The principal regions of parametric resonance are determined numerically from the system of Mathieu equations derived in part I. Results are given for two particular graphite-epoxy shells. The effects of pre-instability inertia in the composite shell is shown to be similar to that discussed previously [2] in connection with isotropic shells. Specifically, it is found that inclusion of pre-instability inertia may result in increased widths of the instability regions of modes having instability forcing frequency very close to a natural frequency of the pre-instability motion of the shell. Also, the effect of pre-instability spatial variation on the principal regions of parametric resonance is separately studied. It is found that the widths of the instability regions may be greatly increased by inclusion of these spatial variations.

1. INTRODUCTION

In part I [1], the theoretical development and solution methodology has been given for the parametric resonance response of a layered anisotropic circular cylindrical shell. The shell is taken to have clamped supports, and is subjected to harmonic axial loading of the form $P^* = (1/2\pi a)(P_0 + P_d \cos \Omega t)$. The unperturbed (pre-instability) response is taken to be a spatially varying state of stress having transverse inertia, rather than a constant membrane state. Fourier series expansions along with a complex periodic form are used to reduce the equations of motion describing the perturbed response to a system of Mathieu equations having the form

$$\underline{m}\frac{\mathrm{d}^2\bar{f}}{\mathrm{d}t^2} + (\underline{R} - P_0\underline{S}_1 - P_d\underline{S}_2 \cos \Omega t)\bar{f} = 0, \tag{1}$$

where $\underline{m}$ is a mass matrix, $\underline{R}$, $\underline{S}_1$ and $\underline{S}_2$ are matrices containing material and geometric constants, and $\bar{f}$ is the vector of unknowns. In the present paper, numerical results are given.

Given such a system of Mathieu equations, dynamic stability can be assessed by a number of methods. Numerous classes of dynamic instability exist. For example, there are first order principal parametric resonances, higher order principal parametric resonances,

0022-460X/93/080323 + 10 $08.00/0

sum combination resonances and difference combination resonances. (The first two are sometimes called direct parametric resonances.) Of the methods available, the monodromy matrix method is the most robust and can determine all instabilities. However, it requires the numerical solution of the differential equations under various sets of initial conditions and is numerically very intensive. Another method due to Hsu (see reference [2]) uses a perturbation procedure and also determines all the instabilities mentioned. However, it is restricted to very small loading. Bolotin's method [3] will not capture the combination resonances but it is fairly straightforward to implement. In the present study, dynamic stability can be assessed by use of the Mathieu equations developed in part I [1] with any of the methods described. Here, the method of Bolotin is used as it is not a goal of this work to present an exhaustive study of all the possible instability regions. Rather, attention is focused on the lower frequency range (up to about five times the overall lowest natural frequency) which is felt to be the range of practical importance. Specifically, prominent instability regions in this range are studied: namely, the first order principal regions of parametric resonance. A major goal of this work is the assessment of the effects of unperturbed response inertia and spatial variation on these instability regions. A study of these effects on other instability regions is a major effort and forms the subject of another paper. It should be noted that these effects have typically been neglected in composite problems (as discussed in reference [1]).

The shells studied are thin and are comprised of orthotropic layers. These layers are taken to be fiber-reinforced composite materials, although the analysis is not restricted to such materials. Results are obtained for graphite–epoxy fiber-matrix material which has a high ratio of longitudinal to transverse stiffness. The properties of this material as well as the geometry of the shell are as follows, where a denotes the radius to the shell's middle surface, l denotes the shell's half-length, h denotes the total thickness of the shell, E denotes Young's modulus, ν denotes the Poisson ratio, G denotes the shear modulus, ρ denotes mass density, subscript l denotes the fiber direction, and subscript t denotes the in-plane direction perpendicular to l: $l/a=1$, $a/h=100$, $E_l=181$ GPa, $E_t=10{\cdot}3$ GPa, $\nu_{lt}=0{\cdot}28$, $G_{lt}=7{\cdot}17$ GPa, $\rho=1600$ kg/m^3. Two laminate configurations, each having three layers, are studied. One laminate has fiber orientations with respect to the axial direction described by 90/0/90 degrees, and the other has 45/−45/45 degrees. All layers have equal thickness and the middle surface lies at the center of the middle layer. Note that since both laminates are symmetrically layered, non-axisymmetric unperturbed response effects are expected to be negligible, as discussed in reference [1].

2. NUMERICAL TECHNIQUES

From equations (1), the static buckling loads P_{cr}, are determined for a particular circumferential wavenumber, k, by the following determinant calculation:

$$\det(\underline{R}-P_{cr}\underline{S}_1)=0. \tag{2}$$

Likewise, the free vibration natural frequencies of the statically loaded shell, ω, are given by

$$\det(\underline{R}-P_0\underline{S}_1-\omega^2\underline{m})=0. \tag{3}$$

As discussed before, the focus here is on determining the boundaries of the principal regions of parametric resonance. By using the methods set forth by Bolotin [3], these are

determined from

$$\det\left(\underline{R} - P_0\underline{S}_1 \pm \tfrac{1}{2}P_d\underline{S}_2 - \tfrac{1}{4}\Omega^2\underline{m}\right) = 0. \tag{4}$$

It should be noted that for each circumferential wavenumber k, a principal region of parametric resonance (first order) exists corresponding to each of the natural frequencies, ω_i. Specifically, for a particular k the region corresponding to the ith natural frequency emanates from $2\omega_i$ at $P_d = 0$.

Determining the numerical values of the determinants in equation (2)–(4) is extremely difficult. The first two problems, equations (2) and (3), can each be converted to an associated eigenvalue problem. This procedure, which is commonly employed, leads to a more readily handled numerical problem. The free vibration natural frequencies of the statically loaded shell, for example, are determined by using

$$(\underline{R} - P_0\underline{S}_1)\bar{f} = \omega\underline{m}\bar{f}.$$

Eigenvalue solver routines in the EISPACK software library are used to compute numerically the eigenvalues associated with each k once the infinite system of Mathieu equations has been truncated. For a typical problem with 20 terms included in the Fourier series expansions, the matrices in the eigenvalue problems are of size 254×254. Computation for one k value takes approximately 18 cpu seconds on an IBM 3090-600E computer system.

The calculation (4) cannot be converted to an eigenvalue problem for Ω because Ω appears as a parameter in $\underline{S}_2$. Direct calculation of the determinant of such a large system is not numerically feasible. Here the system is decomposed via the singular value decomposition theorem which permits the factorization of a real matrix $\underline{M}$ into the form

$$\underline{M} = \underline{A}\underline{S}\underline{B}^{\mathrm{T}},$$

where, T denotes transpose, $\underline{A}$ and $\underline{B}$ are orthogonal matrices, and $\underline{S}$ is a diagonal matrix, the diagonal elements being the so-called singular values of $\underline{M}$. Then, since the determinant of an orthogonal matrix is ± 1, the determinant of $\underline{M}$ is zero when one of the diagonal elements of $\underline{S}$ is zero.

The calculation (4) is thus handled in the following way. It is known that the branches of the principal regions of parametric resonance (first order) emanate from $2\omega_i$ at $P_d = 0$, so one Ω point on each branch is known *a priori*. Subsequent points are determined by increasing P_d by a small amount and searching for the Ω which makes one of the system's singular values zero. Routines in the IMSL software library are used to perform the decomposition.

3. RESULTS

To check the analytical and numerical procedures, several studies were undertaken. The static buckling load of a three-layer glass–epoxy shell was compared with a result by Booton and Tennyson [4]. For a particular laminate configuration the value given in reference [4] is approximately 7820 lb; in the present study the value 7876 lb was calculated. The free vibration natural frequency of a three-layer boron-epoxy shell was compared with a result by Sheinman and Weissman [5]. For a particular laminate, the value given in reference [5] is 2666 rad/s (mode coupling included case); in the present study the value 2664 rad/s was calculated. The parametric resonance forcing frequency of an isotropic shell was compared with a result by Nagai and Yamaki [2]. From Figure 4 of reference [2], the *central frequency* for a particular shell is given as 21·26 (155·91 rad/s) with a

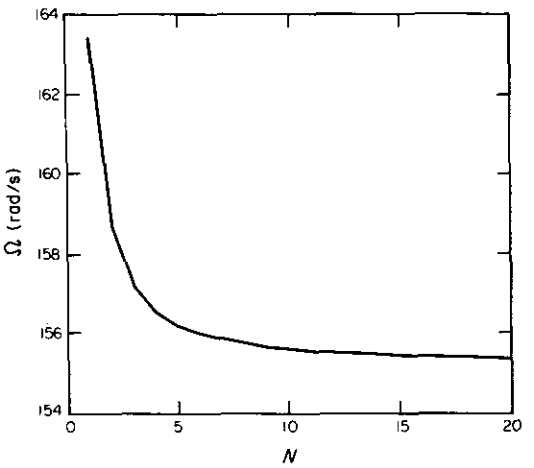

Figure 1. Convergence study for shell of reference [2] with $k=15$.

circumferential wavenumber of 15. In Figure 1, the convergence of the Fourier series expansions is studied for the case taken from reference [2]. N denotes the number of terms taken in the Fourier series summations. The system is seen to have acceptably converged by $N=20$ terms, where the value of Ω is 155·25 rad/s. $N=20$ was used throughout this work and found to be adequate.

Independent results for the parametric resonance of clamped composite shells currently do not exist, and so comparisons were not possible.

For convenience in presenting the subsequent results, load parameters q_0 and q_d related to the overall (for all k) lowest static buckling load, P_{cr_0}, are defined in the following way:

$$P_0 = q_0 P_{cr_0}, \qquad P_d = q_d P_{cr_0}.$$

In Figure 2 the natural frequencies of the 90/0/90 graphite–epoxy shell are presented as functions of k. For this shell $P_{cr_0}=243{\cdot}4$ kN. The shell is loaded with a static load

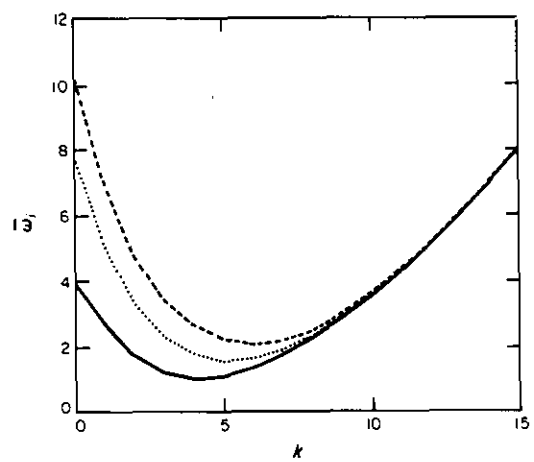

Figure 2. Natural frequencies of the loaded shell; $q_0=0{\cdot}3$; graphite epoxy, 90/0/90. ——, $\bar{\omega}_1$; · · · · ·, $\bar{\omega}_2$; – – –, $\bar{\omega}_3$.

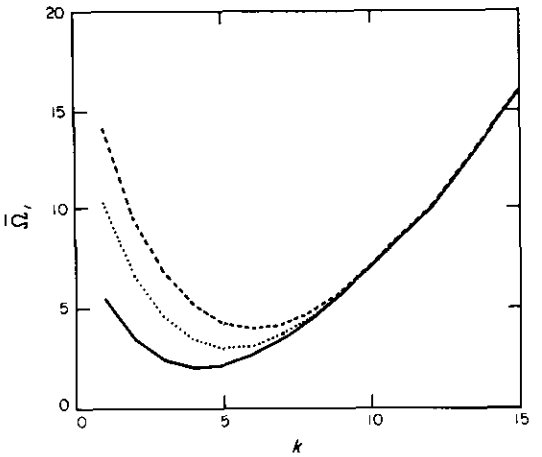

Figure 3. Lower branch values of principal regions of parametric resonance; $q_0=0{\cdot}3$, $q_d=0{\cdot}2$; graphite-epoxy, 90/0/90. ——, $\bar{\Omega}_1$; · · · · ·, $\bar{\Omega}_2$; – – –, $\bar{\Omega}_3$.

$q_0=0{\cdot}3$. $\bar{\omega}_1$, $\bar{\omega}_2$ and $\bar{\omega}_3$ denote the three lowest natural frequencies normalized to the overall lowest value, ω_0. In this case $\omega_0=282{\cdot}5$ rad/s and occurs at $k=4$.

The branches of the first order principal regions of parametric resonance emanate at $q_d=0$ from the values $2\bar{\omega}_i(k)$. In Figure 3 are given the normalized values of the parametric resonance forcing frequencies, $\bar{\Omega}_i$, at $q_d=0{\cdot}2$ on the lower branch emanating from $2\bar{\omega}_i(k)$ as functions of k. Here, and in the sequel, $\bar{\Omega}_i=\Omega_i/\omega_0$. Note that the variation of the lower branch parametric resonance frequency with k is very similar to that of the natural frequency.

In Figure 4 the normalized widths, $\tilde{\Omega}_i$, at $q_d=0{\cdot}2$ of the instability regions are given as functions of k, where,

$$\tilde{\Omega}_i=(\Omega_i^u-\Omega_i^l)/\omega_0,$$

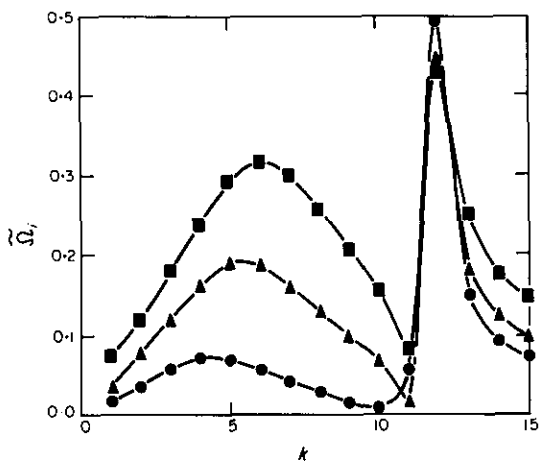

Figure 4. Normalized widths of principal regions of parametric resonance; $q_0=0{\cdot}3$, $q_d=0{\cdot}2$; graphite-epoxy, 90/0/90. ●, $\tilde{\Omega}_1$; ▲, $\tilde{\Omega}_2$; ■, $\tilde{\Omega}_3$.

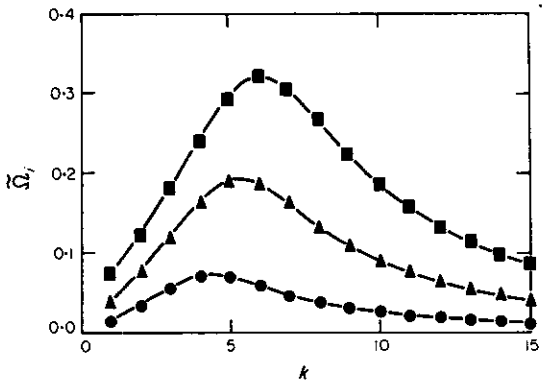

Figure 5. Normalized widths of principal regions of parametric resonance; unperturbed response inertia neglected; $q_0 = 0{\cdot}3$; $q_d = 0{\cdot}2$; graphite-epoxy, 90/0/90. Key as Figure 4.

in which superscripts u and l denote upper and lower branch, respectively. In general, the width of an instability region is of primary importance since it describes a range of frequency over which the shell will be unstable. From Figure 4 it is seen that $\tilde{\Omega}_1$, $\tilde{\Omega}_2$ and $\tilde{\Omega}_3$ have relative maxima at $k=4$, $k=5$, and $k=6$, respectively. Note that these are the k values at which each of the corresponding natural frequencies $\bar{\omega}_1$, $\bar{\omega}_2$ and $\bar{\omega}_3$ attain their respective minima (see Figure 2). In addition, all three curves in Figure 4 show large

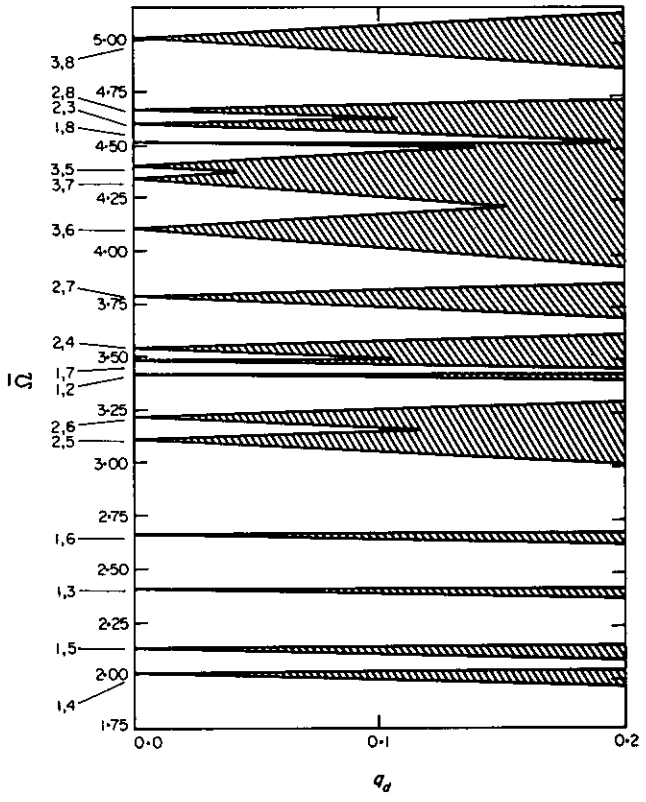

Figure 6. First order principal regions of parametric resonance; $q_0 = 0{\cdot}3$; graphite-epoxy, 90/0/90.

widths at $k=12$. As described in detail in reference [2] (see also [6]) for isotropic shells, this is due to the forcing frequency being very close to one of the shell's unperturbed response natural frequencies. Specifically, here the $q_d=0$ values of $\bar{\Omega}_1$, $\bar{\Omega}_2$ and $\bar{\Omega}_3$ are all very close to the third natural frequency of the unperturbed response, which has the normalized value 10·25. Thus, the same effect of the unperturbed response inertia as observed in isotropic shells is also apparent for composite shells.

For comparison, Figure 5 gives the normalized widths for the same case as Figure 4, except that the unperturbed response inertia is neglected. Note that the unperturbed response spatial variation is retained. For this shell, the two figures are seen to be very similar except in the vicinity of $k=12$.

The first order principal regions of parametric resonance are shown in Figure 6 for a range of frequency up to about five times the overall lowest natural frequency. The numbers on the figure on the left and right of the commas indicate, respectively, frequency mode and circumferential wavenumber. Some of the regions are seen to be quite wide, and some adjacent regions overlap at higher load values.

Next, the role of unperturbed response spatial variation is studied for a shell having fiber orientation given by 45/−45/45. Preliminary numerical work showed that the effects of spatial variation could be significant for this lay-up. Attention is focused on the lower frequency range up to about four times the shell's lowest natural frequency. Other numerical results not presented here show that this range is below the range in which unperturbed response inertia has any significant effect for this shell. For this reason unperturbed response inertia is neglected.

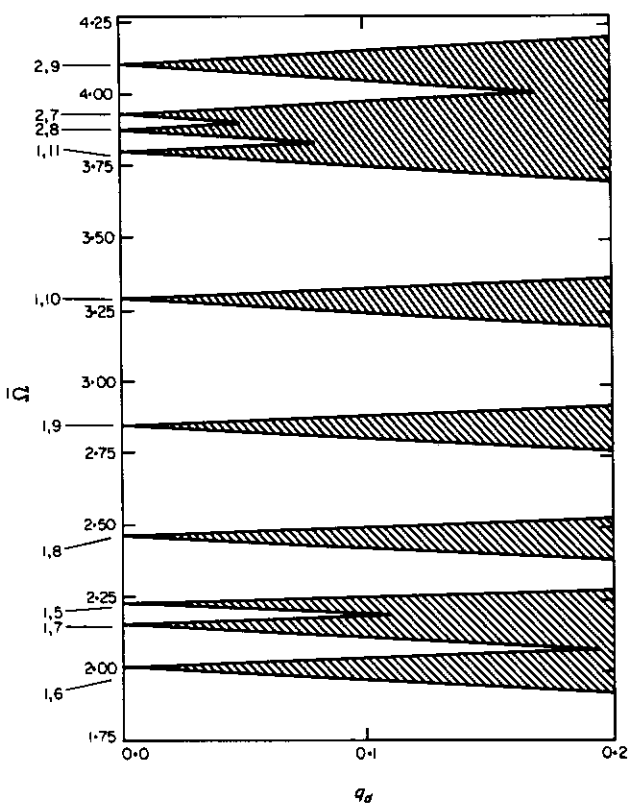

Figure 7. First order principal regions of parametric resonance; unperturbed response inertia neglected; $q_0=0·3$; graphite–epoxy, 45/−45/45.

For this shell $P_{cr_0} = 272{\cdot}7$ kN and $\omega_0 = 281{\cdot}6$ rad/s. In Figure 7 are given the first order principal regions of parametric resonance including unperturbed response spatial variation, and in Figure 8 are given the regions neglecting the spatial variation. For this laminate, the widths of all the regions are seen to be significantly increased by inclusion of the

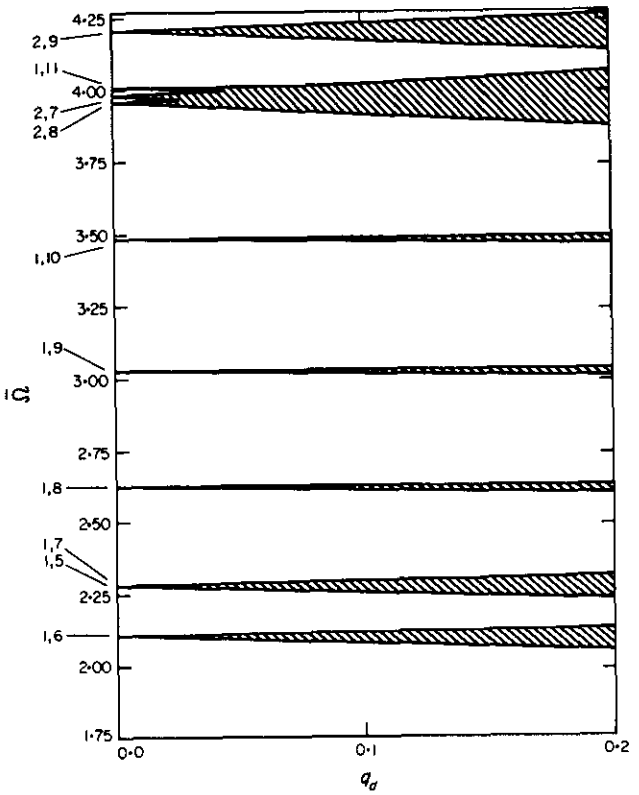

Figure 8. First order principal regions of parametric resonance; unperturbed response inertia and spatial variation neglected; $q_0 = 0{\cdot}3$; graphite–epoxy, 45/−45/45.

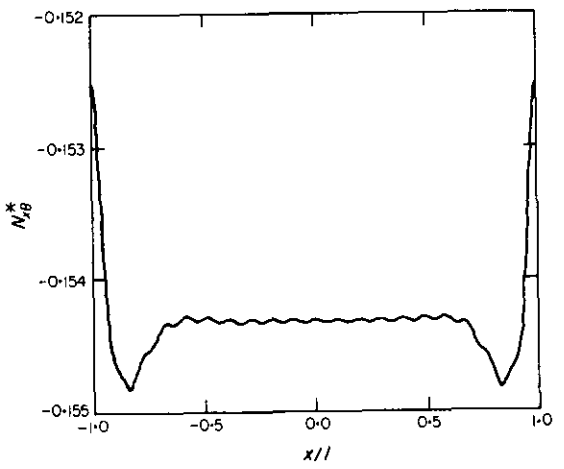

Figure 9. Steady state unperturbed response shear stress resultant; graphite–epoxy, 45/−45/45.

unperturbed response spatial variation. The added instability is induced by significant unperturbed response quantities in the regions of spatial variation near the shell's ends. In Figures 9–12 are shown the relevant unperturbed response quantities in the steady state as functions of the shell's axial co-ordinate, x. (l denotes the shell's half-length.) In the figures,

$$N^*_{x\theta} = N_{x\theta_p}/P^*, \qquad N^*_{\theta\theta} = N_{\theta\theta_p}/P^*, \qquad w^* = w_p E_t/P^*, \qquad w'^* = (\mathrm{d}w_p/\mathrm{d}x)E_t/P^*,$$

where the subscript p denotes the unperturbed response, the N's denote the usual stress resultants, and w denotes the radial displacement component. In Figure 9 the shear stress resultant $N^*_{x\theta}$ is seen to be essentially constant. Also, in Figure 10 the radial displacement component w^* attains its largest value (aside from the two slight bulges) in the central region of the shell, in which w^* is constant. However, in Figures 11 and 12, $N^*_{\theta\theta}$ and w'^*, respectively, are seen to attain significant values in the regions of spatial variation near the shell's ends and so have significant effects in the case in which spatial variations are included.

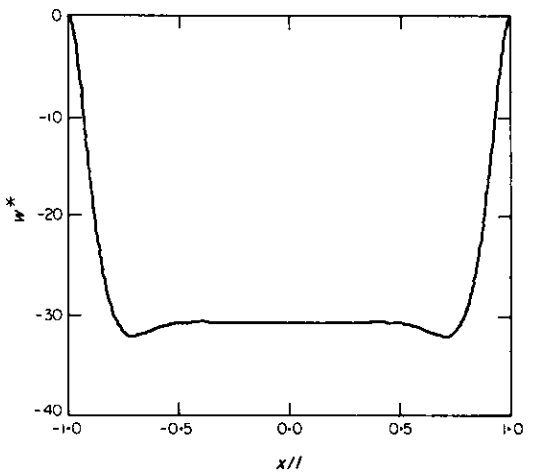

Figure 10. Steady state unperturbed response radial displacement; graphite-epoxy, 45/−45/45.

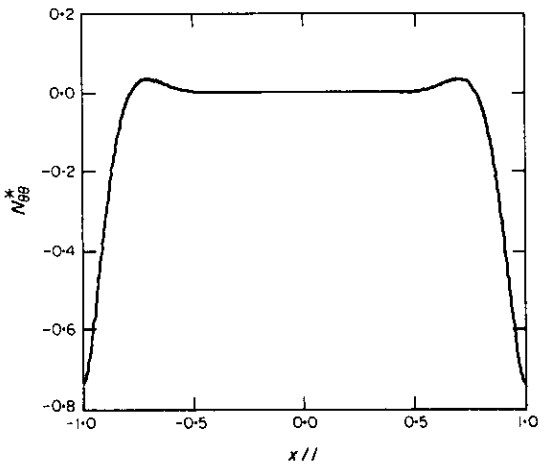

Figure 11. Steady state unperturbed response circumferential stress resultant; graphite-epoxy, 45/−45/45.

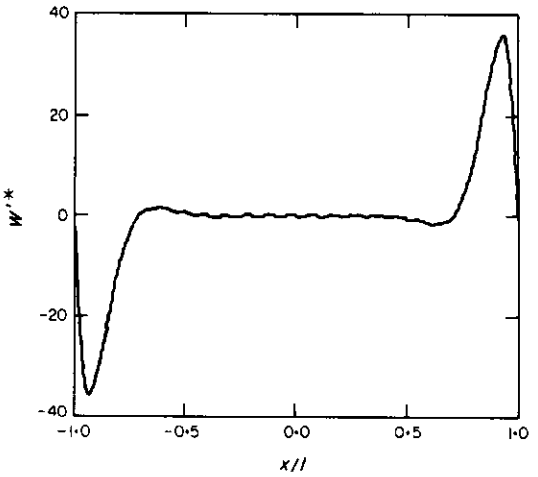

Figure 12. Steady state unperturbed response radial displacement gradient; graphite-epoxy, 45/−45/45.

4. CONCLUSIONS

Numerical results have been presented based on a theoretical analysis given in part I [1]. Dynamic stability diagrams for the first order principal regions of parametric resonance covering about four to five times the lowest natural frequency have been presented for two different layered graphite-epoxy fiber reinforced shells. The role of unperturbed response inertia has been assessed and found to be similar to that in the isotropic shell. Specifically, it was found that instability modes having forcing frequencies near one of the unperturbed response natural frequencies may be greatly effected by the unperturbed response inertia. For the cases of geometry and laminate configuration studied here, other modes were not much affected. The role of the unperturbed response spatial variation was also assessed. For the cases studied here, the widths of the individual instability regions were found to be increased. In particular, the width of the lowest instability region was increased by about 80%. In addition, some adjacent instability regions tended to merge in the spatial variation case, resulting in very wide overall instability regions at higher load values.

REFERENCES

1. A. ARGENTO and R. A. SCOTT 1993 *Journal of Sound and Vibration* **162**, 311–322. Dynamic instability of layered anisotropic circular cylindrical shells, part I: theoretical development.
2. K. NAGAI and N. YAMAKI 1978 *Journal of Sound and Vibration* **58**, 425–441. Dynamic stability of circular cylindrical shells under periodic compressive forces.
3. V. V. BOLOTIN 1964 *The Dynamic Stability of Elastic Systems*. San Francisco: Holden-Day.
4. M. BOOTON and R. C. TENNYSON 1979 *American Institute of Aeronautics and Astronautics Journal* **17**, 278–287. Buckling of imperfect anisotropic circular cylinders under combined loading.
5. I. SHEINMAN and S. WEISSMAN 1988 *Journal of Composite Materials* **21**, 988–1007. Coupling between symmetric and antisymmetric modes in shells of revolution.
6. H. R. RADWAN and J. GENIN 1978 *Journal of Sound and Vibration* **56**, 373–382. Dynamic instability in cylindrical shells.